EUROPEAN ORGANIZATION FOR NUCLEAR RESEARCH

CERN–PPE/96-23
February 19, 1996

A Study of Electron-Muon Pair Production in 450 GeV/c pBe Collisions

T.Åkesson[1,a)], S. Almehed[2)], A.L.S. Angelis[3,b)], J. Antos[1,c)], H. Atherton[1)], P. Aubry[4)], H.W. Bartels[5)], G. Beaudoin[4)], J.M. Beaulieu[4)], H. Beker[1,d)], O. Benary[6)], D. Bettoni[1,e)], V. Bisi[7)], I. Blevis[1,f)], H. Bøggild[1,g)], W.Cleland[8)], M. Clemen[8)], B. Collick[8)], F. Corriveau[9)], S. Dagan[6)], K. Dederichs[1,h)], P. Depommier[4)], N. DiGiacomo[10,i)], S. DiLiberto[11)], J.R. Dodd[3,j)], B. Dolgoshein[12)], A. Drees[5)], S. Eidelman[13)], H. En'yo[1,k)], B. Erlandsson[14)], M.J. Esten[3)], C.W. Fabjan[1)], P. Fischer[5)], A. Gaidot[15)], F. Gibrat-Debu[15)], P. Giubellino[7)], P. Glässel[5)], U. Goerlach[1,l)], Y. Golubkov[12,m)], R. Haglund[2)], L.A. Hamel[9,n)], H. van Hecke[10)], V. Hedberg[1,a)], R. Heifetz[6)], A. Holscher[5)], B. Jacak[10)], G. Jarlskog[2)], S. Johannson[2)], H. Kraner[16)], V. Kroh[5)], F. Lamarche[9,o)], C. Leroy[9,n)], D. Lissauer[16,6)], G. London[15)], B. Lorstad[2)], A. Lounis[4)], F. Martelli[7,p)], A. Marzari-Chiesa[7)], M. Masera[7)], M.A. Mazzoni[1,d)], E. Mazzucato[9,q)], M.L. McCubbin[3,r)], N.A. McCubbin[17)], P. McGaughey[10)], F. Meddi[11)], U. Mjörnmark[2)], M.T. Muciaccia[18)], S. Muraviev[19)], M. Murray[8,s)], M. Neubert[5,r)], P. Nevski[12)], S. Nilsson[14)], L. Olsen[16)], Y. Oren[6)], J.P. Pansart[15)], Y.M. Park[8)], A. Pfeiffer[5)], F. Piuz[1)], V. Polychronakos[16)], P. Pomianowski[8,t)], G. Poulard[1)], M. Price[1)], D. Rahm[16)], L. Ramello[7,u)], L. Riccati[7)], G. Romano[20)], G. Rosa[11,v)], L. Sandor[1,w)], J. Schukraft[1)], M. Sekimoto[1,x)], M. Seman[1,c)], A. Shikonian[19)], A. Shmeleva[19)], V. Sidorov[13)], S. Simone[18)], Y. Sirois[9,y)], H. Sletten[1)], S. Smirnov[12)], W. Sondheim[10)], H.J. Specht[5)], E. Stern[8)], I. Stumer[16)], A. Sumarokov[12,z)], J.W. Sunier[10,+)], V. Tcherniatin[12,aa)], J. Thompson[8)], V. Tikhomirov[19)], C.M. Valine[8)], A. Vanyashin[12,aa)], G. Vasseur[15)], R.J. Veenhof[1,bb)], R. Wigmans[1,cc)], W.J. Willis[1,j)], P. Yepes[9)]

Abstract

We report on the production of $e^{\pm}\mu^{\mp}$ pairs in 450 GeV/c pBe collisions at the CERN SPS. The $e\mu$ signal, which has average missing energy of 21 GeV, is shown to be consistent with expectations from charm decay, and implies a $\sigma \times B$ for $c\bar{c}$ production in p-nucleon collisions of $0.63 \pm 0.28 \mu b$. Alternatively, using an estimate of charm production from other experiments, the data imply a 95% confidence level upper limit of $0.88 \mu b$ on any new physics process which produces $e^{\pm}\mu^{\mp}$.

(to be submitted to Zeit. Phys. C)

[1] CERN, CH-1211 Geneva 23, Switzerland
[2] University of Lund, S-223 62 Lund, Sweden
[3] University College London, London WC1E 6BT, UK
[4] University of Montreal, Montreal, PQ HC3 3J7 Canada
[5] University of Heidelberg, D-69120 Heidelberg, Germany
[6] University of Tel Aviv, Ramat Aviv 69978, Israel
[7] University of Turin and INFN, I-10100 Turin, Italy
[8] University of Pittsburgh, Pittsburgh PA 15260, USA
[9] McGill University, Montreal, PQ H3A 2T8 Canada
[10] Los Alamos National Laboratory, Los Alamos, NM87544, USA
[11] University of Rome 'La Sapienza' and INFN, I-00185 Rome, Italy
[12] Institute of Physics and Engineering, RU-115409 Moscow, Russia
[13] Institute of Nuclear Physics, RU-630090 Novosibirsk, Russia
[14] University of Stockholm, S-11346 Stockholm, Sweden
[15] DAPNIA, CE Saclay, F-91191 Gif-sur-Yvette, France
[16] Brookhaven National Laboratory, Upton, NY 11973, USA
[17] Rutherford Appleton Laboratory, Didcot OX11 0QX, UK
[18] University of Bari and INFN, I-70100 Bari, Italy
[19] Lebedev Institute of Physics, RU-117924 Moscow, Russia
[20] University of Salerno and INFN, I-84100 Salerno, Italy
[a] Now at: University of Lund, S-223 62 Lund, Sweden
[b] Now at: University of Geneva, CH-1211 Geneva 4, Switzerland
[c] Visitor at CERN from Slovak Academy of Sciences, SQ-04353 Kosice, Slovak Republic
[d] Now at: University of Rome 'La Sapienza' and INFN, I-00185 Rome, Italy
[e] Now at: University of Ferrara and INFN, I-44100 Ferrara, Italy
[f] Visitor at CERN from Weizmann Institute, Rehovot, Israel
[g] Visitor at CERN from Niels Bohr Institute, DK-2100 Copenhagen Ø, Denmark
[h] Visitor at CERN from Ludwig-Maximilians-Universität, D-80539 München, Germany
[i] Now at: SAIC, San Diego, USA
[j] Now at: University of Columbia, Nevis Labs., NY 10533, USA
[k] Now at: University of Kyoto, Kyoto 606, Japan
[l] Now at: University Louis Pasteur, F-67200 Strasbourg, France
[m] Now at: Moscow State University, RU-117234 Moscow, Russia
[n] Now at: University of Montreal, Montreal, PQ HC3 3J7 Canada
[o] Now at: LeCroy, Chesnut Ridge, NY 10977-6499, USA
[p] Now at: University of Urbino, I-61029 Urbino, Italy
[q] Now at: DAPNIA, CE Saclay, F-91191 Gif-sur-Yvette, France
[r] Now at: CERN, CH-1211 Geneva 23, Switzerland
[s] Now at: Texas A&M University, MS-3366, TX 77843, USA
[t] Now at: Virginia Polytechnic Institute, Blacksburg VA 24061
[u] Now at: Politecnico of Milan, I-20100 Milan, Italy
[v] Now at: University of Salerno and INFN, I-84100 Salerno, Italy
[w] Now at: Slovak Academy of Sciences, SQ-04353 Kosice, Slovak Republic
[x] Visitor at CERN from Institute of Nuclear Study, Tokyo 188, Japan
[y] Now at: Ecole Polytechnique, F-91128 Palaiseau, France
[z] Now at: Institute of Physics, Acad. Sinica, Taipei 11529, Taiwan
[aa] Now at: Brookhaven National Laboratory, Upton, NY 11973, USA
[bb] Visitor at CERN from NIKHEF-H, NL-1009 DB Amsterdam, the Netherlands
Now at: LIP, P-1000 Lisboa, Portugal
[cc] Now at: Texas Tech. University, Lubbock TX 79409, USA
[+] Deceased

1 Introduction

The HELIOS spectrometer has been used to measure the production of centrally produced $e^{\pm}\mu^{\mp}$ pairs in pBe collisions at 450 GeV/c at the CERN SPS. The measurement of the leptons is complemented by a calorimetric measurement of the total energy, and hence of any 'missing' energy. The production of $e^{\pm}\mu^{\mp}$ pairs is of interest because:

- it is sensitive to open-charm production through the semi-leptonic decay of both charmed hadrons. Hadro-production of charm has been challenging for both experiment and theory, particularly in the SPS energy range where the charm cross-section is rising quickly [1]. The particular advantage of the $e\mu$ channel is that it avoids all hadronic decays which feed the di-electron and di-muon channels.
- $e^{\pm}\mu^{\mp}$ pair production in excess of the contribution from the standard model (essentially charm) would indicate new physics.

There has been no previous study of hadronically produced $e\mu$ pairs with missing energy at fixed target energies. The HELIOS apparatus is ideally suited for this study because of its ability to identify promptly produced electrons and muons, and its hermetic 4π calorimetry. It was designed to study lepton pairs in the low mass (≤ 1 GeV) and low transverse momentum region. The 4π calorimetry provides an energy resolution of 18 GeV on the total event energy of 450 GeV. This resolution is adequate to observe the missing energy (average value about 21 GeV) expected from $c\bar{c}$ double semi-leptonic decay. In the analysis reported here, we have extracted a signal of $e^{\pm}\mu^{\mp}$ pairs which are found to have large missing energy. Apart from charm, at our energy ($\sqrt{s}$ of 29 GeV for the proton-nucleon collision) only correlated K^+K^- pairs, where one kaon decays to $\mu\nu$ and the other to $\pi e\nu$, contribute to an $e\mu$ signal with large missing energy. We show that the contribution of K^+K^- pairs is small, and hence obtain a measurement of:

$$\sigma(c\bar{c})\,[B(c \to e^+X)B(\bar{c} \to \mu^-X) + B(\bar{c} \to e^-X)B(c \to \mu^+X)].$$

Alternatively, taking the charm cross-section from other experiments, we can use our data to set an upper limit on any new source of $e\mu$ pairs.

In Section 2 the HELIOS apparatus and data taking are briefly discussed. Section 3 discusses event reconstruction and selection. Section 4 shows the results of modelling the data with Monte Carlo simulated data, and in Section 5 the results are presented: an estimation of the charm cross section, and an upper limit on new sources of $e\mu$ signal.

2 Apparatus, Triggering, and Data-Taking

The HELIOS spectrometer, which operated in the H8 beam line of the CERN SPS North Area, is shown in Figure 1. The spectrometer combines electron identification, muon identification, and measurement of the total energy of the event. A full description of the detector components and triggering may be found in [2] and references therein. We give here only a brief summary of the features essential to the present analysis.

A 450 GeV/c proton beam is focused on to a 4cm long thin (125μm diameter) beryllium wire target. In the 'Electron spectrometer', charged particle tracking and momentum information is obtained from the three drift chambers (DC1, DC2, and DC3) positioned before and after the calorimetrized dipole magnet (MAGCAL). The electron trigger requires a coincidence of signals from the silicon pad array close to the target, the transition radiation detector (TRD), and the uranium/liquid argon calorimeter (ULAC). In the 'Muon spectrometer', track and momentum reconstruction makes use of the seven proportional chambers (PC0 to PC6) and the Muon magnet. The muon trigger requires matching hits in the scintillator hodoscopes (H3 and H2) on either side of the Iron wall,

and a track in the trigger planes of the proportional chambers (PC3 to PC6) downstream of the Muon magnet.

Hermetic calorimetry provides a measurement of the total energy in the event. The target region is surrounded by Fe/scintillator, U/scintillator, and U/Cu/scintillator calorimeter modules, covering the region of polar angle 6.3° (η_{lab} = 2.9) to 95.7° (η_{lab} = -0.1), and by the ULAC in the forward region ($\eta_{lab} > 2.9$), where most of the event energy is deposited. The ULAC is divided into an 18 radiation length electromagnetic section with tower readout, and a 4.5 interaction length hadronic section with interleaved strip readout. Additional U/scintillator modules ('BEAM' and 'VETO' in Figure 1) behind the ULAC give a total of 10.3 interaction length sensitive depth along the beam direction.

This analysis uses three triggered data samples taken during the 1989 run: di-electron ($e \cdot e$), di-muon ($\mu \cdot \mu$), and electron-muon ($e \cdot \mu$) triggered data. In addition a sample of 'minimum bias' events was taken, for studies of detector performance and monitoring. The di-electron and di-muon data, with their well-known resonance peaks, are used to test the reconstruction of electrons and muons, as well as to provide normalization of the $e\mu$ signal. To ensure proper normalization, only data taken when all three di-lepton triggers were operational are used in the analysis, corresponding to approximately $2 \times 10^6 e \cdot e$, $1.5 \times 10^6 \mu \cdot \mu$, and $1 \times 10^6 e \cdot \mu$ triggers.

3 Event Reconstruction and Selection

3.1 Standard Reconstruction Techniques

Full details of event reconstruction may be found elsewhere [2, 3]. The main points are as follows. Events in which hadronic particles leak through into the muon spectrometer are removed by a cut on multiplicity in the first two muon chambers PC0 and PC1. Muon reconstruction requires that a track reconstructed in the muon spectrometer should have a momentum greater than 7 GeV/c, and should match a track found in the drift chambers of the electron spectrometer. This matching improves significantly the resolution on the production angle at the target and rejects muons produced downstream [4]. Electron reconstruction requires that an isolated electromagnetic ULAC shower should be matched spatially and energetically with a drift chamber track. Furthermore, there should be no signals in the ULAC or TRD which could be due to a conversion partner. The electron track is required to have a momentum greater than 3 GeV/c.

The total energy in the event is obtained from the flash ADC readout of the calorimeters. The ADC system also incorporates an array of sampling 'history' ADC modules which provide information on the time evolution of pulses over $\sim 1\mu$sec in each element of the calorimetry. This information is used off-line to discard events which show evidence of energy 'pile-up' from neighbouring interactions. Events with large energy ($\geq$ 6 GeV) in the VETO calorimeter, indicating poor containment of event energy, are also discarded. Further details on the use of the calorimeter information may be found in [5]. The total energy resolution obtained from the calorimeter flash ADCs for minimum bias events is σ_{Etot} = 18 GeV. A major contribution to this overall resolution comes from the systematics of combining several different types of calorimeter.

After the event reconstruction and selection described above, the di-electron and di-muon data, shown in Figures 2 (a) and 2 (b) respectively, show clear evidence of the ρ/ω resonance peak. A strong ϕ peak is also evident in the $\mu\mu$ data, as well as a J/ψ peak (see inset of Figure 2 (b)). However, at this stage of the analysis, any $e\mu$ signal still has a substantial background, as shown in Figure 3. Defining background (B) as the total number of $e^+\mu^+$ and $e^-\mu^-$ pairs, and signal (S) as $e^\pm\mu^\mp$−B, then at this stage S= 99 ± 44

pairs, with a signal to background of 0.11.

3.2 Electron - Muon Signal Optimisation

Table 1: Effect of Drift Chamber and Momentum Cut on $e\mu$ Data

Cut	$e^{\pm}\mu^{\mp}$Pairs	B=$e^{+}\mu^{+} + e^{-}\mu^{-}$	S=$e^{\pm}\mu^{\mp}$−B	S / B
Momentum Requirement: $P_e \geq 3, P_\mu \geq 7$ GeV/c				
DC23	1023 ± 32	924 ± 30 (100%)	99 ± 44 (100%)	0.11
DC123	553 ± 24	471 ± 22 (51%)	82 ± 32 (83%)	0.17
Momentum Requirement: $P_e \geq 7, P_\mu \geq 7$ GeV/c				
DC23	361 ± 19	260 ± 16 (28%)	101 ± 25 (102%)	0.39
DC123	205 ± 14	119 ± 11 (13%)	86 ± 18 (87%)	0.72

Monte Carlo studies of charm production have been made to try to find kinematic cuts which should enhance the signal to background. The Monte Carlo package used consists of Pythia (version 5.3) and Jetset (version 7.2) [6] to simulate hadron-hadron scattering and fragmentation, followed by the standard HELIOS detector Monte Carlo program for the trigger and detector response. Decays of ρ, ω, and ϕ into both the ee and $\mu\mu$ channels were used to ensure that the apparatus Monte Carlo program reproduced accurately the acceptance, efficiency, and resolution of the real apparatus, particularly the energy resolution. Once this was done, no further adjustments were made to the Monte Carlo.

The Monte Carlo predicted that, as might be expected, leptons from charm decay have a harder momentum spectrum than leptons from other sources. Accordingly the cut on the electron momentum was raised from 3 GeV/c to 7 GeV/c to match the muon lower limit.

In addition all tracks are required to have a segment found in DC1, the drift chamber in front of the MAGCAL. This requirement introduces some inefficiency, as DC1 sees the highest track density, but it helps to remove biases between the ee, $\mu\mu$, and $e\mu$ samples, as well as non-prompt leptons, particularly muons from pion and kaon decays.

Two other cuts have been applied at this stage to remove biases between the different di-lepton samples as well as to ensure agreement between data and Monte Carlo simulations. All pair types are required to have an opening angle before the MAGCAL of greater than 30mrad. This cut is introduced firstly because one component of the electron trigger vetos close pairs, which removes conversions, and secondly it avoids close track pairs in DC1. Also, as the ee analysis requires the two leptons to be separated by at least 6 cm at the ULAC front face, this requirement is imposed on all lepton pairs.

The effects of the momentum cut and DC1 requirement on the signal, with all other cuts applied, are shown in Table 1. The final cuts used give a signal of 86 ± 18 events, with a signal to background of 0.72.

4 Analysis of Signal

4.1 Event Energy

If the total energy measured in the event is less than the 450 GeV expected, the missing energy indicates the production of neutrinos. The event selection described above does not cut on missing energy. Rather, after events are selected, the energy spectrum of

the signal can be examined for evidence of neutrino production. The energy resolution is known to be 18 GeV for minimum bias events, with no missing energy seen. Events containing neutrino-less decays of resonances should show a similar energy spectrum. This is confirmed in Figures 4 (a) and 4 (b), which show no missing energy from events containing ρ/ω di-lepton pairs, with the expected energy resolution. However, the $e\mu$ signal shows an average of 21 GeV of missing energy, a clear indication of neutrino production, as seen in Figure 5. The figure also shows the data agree with the shape of the Monte Carlo prediction from the double semi-leptonic decay of a $c\bar{c}$ pair, as will be discussed fully in the following sections.

4.2 Monte Carlo Studies

As mentioned in section 3.2, the Monte Carlo chain consists of Pythia (5.3) and Jetset (7.2) followed by the standard HELIOS detector Monte Carlo, and was tuned to describe the ρ, ω, and ϕ resonances seen in the data. Results from the Monte Carlo are used for the following purposes:

- to suggest kinematic cuts which might improve the signal, as discussed previously in section 3.2;
- to provide information which can be used, together with the data, to estimate the "correlated" K^+K^- component in the data, as discussed in the next section;
- to provide predictions for the $e\mu$ signal which can be compared to data;
- to furnish the factors which allow extrapolation of the cross-section in the region covered by the detector to the total cross-section integrated over the full phase space.

It was checked that the Monte Carlo gives a good description of the shape and, where possible, the magnitude of the mass distributions of the various like-sign pair combinations.

4.3 Estimation of K^+K^- Contribution to Signal

While many channels can produce $e\mu$ pairs with missing energy (e.g. $K^+ \to \mu^+\nu, \pi^- \to \pi^o e^-\nu$), most of these are removed by appropriate subtraction of like-sign pairs, and so do not contribute to the "signal". Besides $c\bar{c}$ decay, at $\sqrt{s}$ of 29 GeV the Standard Model allows only decays from "correlated" K^+K^- production (i.e. produced from a single $s\bar{s}$ pair) to contribute a substantial $e\mu$ signal. The Monte Carlo predicts an average missing energy from K^+K^- decay of 15 GeV, so we cannot distinguish this channel using missing energy.

We estimate the maximum contribution as follows. Assuming that all $K \to \mu\nu$ and $K \to \pi\mu\nu$ decays produce reconstructed muons, the Monte Carlo predicts that 7.4% of the like-sign di-muons seen in the data are produced through $K^\pm K^\pm \to \mu^\pm\mu^\pm$. (Such like-sign K's are of course "uncorrelated".) The number of $\mu^\pm\mu^\pm$ events seen in the data is 177, and so the number of uncorrelated K's is $0.074 \times 177 = 13$ events. The Monte Carlo also predicts that the "uncorrelated" contribution of $K^\pm K^\mp$ decay to $\mu^+\mu^-$ should be a little larger, 15 events, and that the "correlated" contribution should be 1.5 times the "uncorrelated", i.e. 23 events. Finally, to get the correlated contribution to $e\mu$, allowance must be made for the difference in branching ratio (reduction of a factor of 7 for $KK \to e\mu$ compared to $\mu\mu$) and smaller total acceptance for e's (reduction of a factor of 2). This reduces the expected $K^\pm\ K^\mp \to e^\pm\ \mu^\mp$ yield to at most 2 events, or 2% of the $e\mu$ signal.

4.4 Comparison of $e\mu$ Signal to Charm

Having found that the $K^{\pm}\ K^{\mp}$ contribution is negligible, it remains to compare the observed signal to that expected from associated charm production. The kinematic distributions predicted by the Monte Carlo chain show good agreement with the $e\mu$ signal, as seen in Figures 5, 6, and 7. All plots have a common normalization factor: the total number of Monte Carlo events is normalised to the signal of 86 events.

The comparison between data and Monte Carlo for all the points in Figures 5, 6, and 7 shows reasonably good agreement in all variables. Of particular significance is the large missing energy associated with these events. The mean missing energy of 21 GeV in the $e\mu$ signal events agrees with the Monte Carlo expectation for the semi-leptonic decay of charm. Although the statistics are small, this indicates that the signal does not have a large component of pairs produced with less or no missing energy.

The agreement in shape between the data and Monte Carlo spectra, as well as the good signal to noise ratio, all support the interpretation that a clean sample of $e\mu$ pairs from charm decay has been selected.

5 Results

5.1 Estimation of Charm Cross Section

The extraction of the $e\mu$ signal, and its agreement with the Pythia 5.3 Monte Carlo expectations from charm production and decay, have been shown in the previous sections. Depending on selection criteria, the resulting signal (see Table 1) is $2\ -\ 3$ times larger than previously published data in hadro-production at $\sqrt{s} \sim 30\,\mathrm{GeV}$ [7].

This clean sample of charm decays can now be used to obtain a cross section measurement for $pp \to c\bar{c}$ production, or, using other measurements of charm production, to place a limit on new physics processes with an $e\mu$ decay mode. The cross section can be expressed by:

$$\sigma(c\bar{c} \to e^{\pm}\mu^{\mp}X) = N_{(c\bar{c}\to e^{\pm}\mu^{\mp}\ seen)} \times \frac{\sigma_{inelastic}}{N_{interactions}} \times \frac{1}{A^{\alpha_{charm}}} \times \frac{1}{\varepsilon(c\bar{c} \to e\mu)} \qquad (1)$$

where

- $\sigma(c\bar{c} \to e^{\pm}\mu^{\mp}X) = \sigma_{c\bar{c}} \times [B(c \to e^{+}X)B(\bar{c} \to \mu^{-}X) + B(\bar{c} \to e^{-}X)B(c \to \mu^{+}X)]$. $\sigma_{c\bar{c}}$ is the total cross section (integrated over all phase space) for $c\bar{c}$ production in pp collisions, and $B(c \to e^{+}X)$ is the inclusive semi-electronic branching ratio of c to e^{+} (with similar notation for other branching ratios);
- $N_{(c\bar{c}\to e^{\pm}\mu^{\mp}\ seen)}$ is the number of signal events in the data;
- $\sigma_{inelastic}$ is the total pp inelastic cross section;
- $N_{interactions}$ is the number of inelastic pBe interactions;
- $A^{\alpha_{charm}}$ is the atomic mass dependence of the $c\bar{c}$ production cross-section in the phase space region covered by the detector;
- and $\varepsilon(c\bar{c} \to e\mu)$ is an absolute efficiency factor, including trigger, reconstruction, and acceptance. It includes the factor which extrapolates from the phase space region covered by the detector to the full phase space, as given by the pp Monte Carlo.

Because $N_{interactions}$ and the absolute efficiency are not well known, this equation cannot be used as it stands. However, a precisely analogous equation can be written for the ρ/ω resonance:

$$\sigma_{\rho/\omega} \times B(\rho/\omega \to l^{+}l^{-}) = N_{(\rho/\omega\to l^{+}l^{-}\ seen)} \times \frac{\sigma_{inelastic}}{N_{interactions}} \times \frac{1}{A^{\alpha_{\rho/\omega}}} \times \frac{1}{\varepsilon(\rho/\omega \to l^{+}l^{-})} \qquad (2)$$

where

$$\sigma_{\rho/\omega} \times B(\rho/\omega \to l^{+}l^{-}) = \sigma_{\rho}\ B(\rho \to l^{+}l^{-}) + \sigma_{\omega}\ B(\omega \to l^{+}l^{-}). \qquad (3)$$

Since the cross-sections and branching ratios for the ρ and ω are reasonably well-determined, these resonances can be used for normalization.

First, the ratio:

$$\mathcal{R}_{(l^+l^-)} = \frac{N_{(\rho/\omega \to l^+l^- \ seen)}}{\sigma_{\rho/\omega} \ B(\rho/\omega \to l^+l^-)} \tag{4}$$

can be evaluated for e^+e^- and $\mu^+\mu^-$ separately. Combining this equation with Equations (3) and (4) gives:

$$\sqrt{\mathcal{R}_{(e^+e^-)}\mathcal{R}_{(\mu^+\mu^-)}} = \frac{N_{interactions}}{\sigma_{inelastic}} \times A^{\alpha_{\rho/\omega}} \times \sqrt{\varepsilon(\rho/\omega \to e^+e^-)\varepsilon(\rho/\omega \to \mu^+\mu^-)} \tag{5}$$

and, finally, eliminating $N_{interactions}/\sigma_{inelastic}$ from Equation (1) gives:

$$\sigma(c\bar{c} \to e^\pm\mu^\mp X) = N_{(c\bar{c}\to e^\pm\mu^\mp \ seen)} \times \frac{1}{\sqrt{\mathcal{R}_{(e^+e^-)}\mathcal{R}_{(\mu^+\mu^-)}}} \times \frac{A^{\alpha_{\rho/\omega}}}{A^{\alpha_{charm}}} \times \frac{\sqrt{\varepsilon(\rho/\omega \to e^+e^-)\varepsilon(\rho/\omega \to \mu^+\mu^-)}}{\varepsilon(c\bar{c} \to e\mu)}. \tag{6}$$

We now consider the various terms on the right-hand side of Equation (6). In order to evaluate $\mathcal{R}_{(e^+e^-)}$ and $\mathcal{R}_{(\mu^+\mu^-)}$ using Equation (4), first the number of ρ/ω events in the data must be determined. This is done by fitting the observed mass spectra to a combination of a Lorentzian line-shape for the ρ and a Gaussian for the ω. (The mass resolution, FWHM, in both e^+e^- and $\mu^+\mu^-$ is smaller than the ρ width, but larger than the ω.) Because the relative ρ and ω contributions to the yield cannot be determined from the fit, this ratio is obtained from Monte Carlo, assuming equal production cross-sections and using branching ratios from [9]. In addition a linear background term is allowed in the case of $\mu^+\mu^-$ pairs. A study of the full 1989 di-muon sample showed evidence for destructive interference between the ρ and ω ([2] and references therein) with the result that the number of events seen in the data should be increased by 15% to correspond to the sum of cross-sections as used in Equations (3) and (4). This 15% correction has been applied, with a corresponding increase in the systematic error. The results of the fits, including the 15% interference correction, are:

$$N_{(\rho/\omega \to e^+e^- \ seen)} = 46 \pm 26$$
$$N_{(\rho/\omega \to \mu^+\mu^- \ seen)} = 110 \pm 59.$$

Next, cross-sections and branching ratios taken from [8]and [9] respectively [1] give:

$$\sigma_\rho \ B(\rho \to e^+e^-) + \sigma_\omega \ B(\omega \to e^+e^-) = 1.55 \pm 0.08 \mu b$$
$$\sigma_\rho \ B(\rho \to \mu^+\mu^-) + \sigma_\omega \ B(\omega \to \mu^+\mu^-) = 1.57 \pm 0.08 \mu b$$

and so, from Equation (4):

$$\mathcal{R}_{(e^+e^-)} = 30 \pm 17 \mu b^{-1}$$
$$\mathcal{R}_{(\mu^+\mu^-)} = 70 \pm 38 \mu b^{-1}.$$

The next term in Equation (6) is the ratio of the A^α dependences for ρ/ω and charm. For central ρ/ω production $\alpha = 0.72 \pm 0.01$ [10], and for central charm production $\alpha = 1.02 \pm 0.04$ [11] for charm.

The final term in Equation (6) is a ratio of overall efficiencies. Here care has been taken to ensure as much cancellation as possible. For example, the efficiency of reconstructing an electron-muon pair coming from $c\bar{c}$ decay, $\varepsilon(c\bar{c} \to e\mu)$, includes the product

[1] Because the branching ratio $B(\omega \to \mu^+\mu^-)$ is not well-measured, we assume $B(\omega \to \mu^+\mu^-) = B(\omega \to e^+e^-)$

of the single electron and single muon trigger efficiencies. However, the numerator includes the di-electron and di-muon trigger efficiencies. The di-muon trigger efficiency is identical to the product of two single muon trigger efficiencies, leading to cancellation of the muon trigger efficiency in Equation (6). Unlike the di-muon trigger, the di-electron trigger requires, in addition to two single electron triggers, a veto in cases where the two candidates are close together [2]. To correct for this in the present analysis, a spatial separation of 6 cm at the ULAC face, determined from a Monte Carlo simulation of the electron trigger, has been required off-line for all pairs, ensuring this additional veto had no effect - see also section 3.2. This off-line cut restores cancellation of the electron trigger efficiencies in Equation (6).

The efficiency ratio term is still not 1, because $e\mu$ pairs from charm are produced over a very broad mass range (about $0.2 - 2.0\,\mathrm{GeV/c^2}$) and the reconstruction efficiency is mass dependent. Also the characteristics of charm and ρ/ω production are different, so the ratio of the factors which extrapolate from the central region in which we have data to total cross-section also enters here. (Hence we are assuming that the *shapes* of the relevant production spectra are well described by Pythia and Jetset.) All these effects are included in the Monte Carlo and lead to a value for the last term in Equation (6) of 0.65.

With all the necessary restrictions in place, 86 ± 18 $e^{\pm}\mu^{\mp}$ events have been retained, yielding:

$$\sigma(c\bar{c} \rightarrow e^{\pm}\mu^{\mp}X) = 0.63 \pm 0.25(stat.) \pm 0.13(syst.)\mu b.$$

The largest contribution to the systematic error is the 15% from the ρ/ω interference. Various smaller effects lead to a total systematic error of 20% compared to the 40% statistical error.

As a check, the entire analysis has also been carried out with the electron momentum cut relaxed from 7 GeV/c to 3 GeV/c. The result obtained is consistent within errors.

To estimate the $c\bar{c}$ cross section, a value for $B(c\bar{c} \rightarrow e^{\pm}\mu^{\mp}X)$ is required, and this depends on the relative production of the various charmed hadrons. Faced with a similar problem, the E653 collaboration [12] have estimated that in 600 GeV/c π^- emulsion collisions the inclusive semi-muonic branching ratio $B(c \rightarrow \mu)$ is $9.3 \pm 1.3\%$, which is dominated by the systematic error. This is similar to the value obtained in e^+e^- collisions; see [13] and references therein. Using the E653 value, and assuming the same value for the electron branching ratio, leads to $B(c\bar{c} \rightarrow e^{\pm}\mu^{\mp}X) = 1.7 \pm 0.3\%$, and hence:

$$\sigma_{c\bar{c}} = 37 \pm 18 \mu b$$

where statistical and systematic errors have been combined in quadrature.

5.2 Upper Limit on New Physics

We have obtained $\sigma \times B = 0.63 \pm 0.28 \mu b$ (statistical and systematic errors added in quadrature) for the production of a source of $e^{\pm}\mu^{\mp}$ pairs with the production and decay characteristics of charm. The EHS collaboration has obtained $14.6 \pm 2.0 \mu b$ for $\sigma(D\bar{D})$ in pp collisions at 400 GeV/c [14], where D is D^0 or D^+. Using the relative production rates of D^0, D^+, D_s, and Λ_c as estimated by E653 [12] implies that $D\bar{D}$ is $44 \pm 7\%$ of $c\bar{c}$ production. Thus the EHS measurement implies $\sigma(c\bar{c} \rightarrow e^{\pm}\mu^{\mp}X) = (14.6/0.44) \times 0.017 = 0.56 \pm 0.15 \mu b$. Our value is entirely consistent with this.

While we have shown that the signal observed is completely compatible with charm, we may also use our cross-section and that derived from the EHS measurement to set

an upper limit on any new source of $e^{\pm}\mu^{\mp}$ pairs. Using the algorithm described by the PDG [9], we obtain an upper limit of $0.88\mu b$ at 95% confidence.

6 Conclusions

We have observed a signal of centrally produced $e^{\pm}\mu^{\mp}$ pairs in pBe collisions at 450 GeV/c. At most 2% of the signal comes from strangeness production. The kinematic distributions predicted by the Pythia 5.3 Monte Carlo for the associated production of open charm, with each charmed hadron decaying semi-leptonically, show good agreement with the $e\mu$ signal. In particular the $e\mu$ signal shows a mean missing energy of 21 GeV, in agreement with the Monte Carlo prediction for charm. Hence electron-muon pairs would seem to be an excellent way to study inclusive charm production.

The signal implies a total cross-section in 450 GeV/c pp collisions of:

$$\sigma(c\bar{c} \rightarrow e^{\pm}\mu^{\mp}X) = 0.63 \pm 0.25(stat.) \pm 0.13(syst.)\mu b.$$

Comparing the above value to one which may be derived from the EHS data, we obtain an upper limit at 95% confidence level on unexpected physics processes decaying through a correlated $e^{\pm}\mu^{\mp}$ channel of 0.88 μb, or approximately equal to the contribution from charm.

7 Acknowledgements

The HELIOS collaboration wishes to express its thanks for the excellent work of the staff of the PS-SPS accelerator complex, and of the technical staff at CERN and the collaborating institutes. The support of the research councils and funding agencies in our home countries is also acknowledged. Special acknowledgment is given to the U.S. DOE and Pittsburgh Supercomputing Center (NSF/PSC Grant PHY860008P).

References

[1] See for example J. Appel, Ann. Rev. Nuclear and Particle Science 42 (1992) 367, and J. Cumalat, Proceedings of XXVII Int. Conf. on High Energy Physics, Glasgow 1994, Volume 1, p.255.
[2] T. Åkesson et al., Z.Phys. C68 (1995) 47.
[3] P. Pomianowski, PhD thesis, University of Pittsburgh USA (1994).
[4] R.J. Veenhof, PhD thesis, Universiteit van Amsterdam Nederland (1993).
[5] T. Åkesson et al., Z.Phys. C52 (1991) 219.
[6] The Lund Monte Carlo Programs, CERN long writeup (1989).
[7] A.G.Clark et al., Phys. Lett. B77 (1978) 337.
[8] Numbers used for ρ/ω cross sections taken from: M. Aguilar-Benitez et al. Z.Phys. C50 (1991) 405. Values have been scaled to $\sqrt{s} = 29$ GeV using the Bourquin-Gaillard parametrization, Nucl. Phys. B114 (1976) 334.
[9] Review of Particle Properties, Phys. Rev. D45 (1992).
[10] M. Binkley et al., Phys. Rev. Lett. 37 (1976) 571.
[11] M. J. Leitch et al., Phys. Rev. Lett. 72 (1994) 2542.
[12] K. Kodama et al., Phys. Lett. B 284 (1992) 461. We are grateful to C. Zhang for bringing this publication to our attention.
[13] H. Albrecht et al., Phys. Lett. B 278 (1992) 202.
[14] M. Aguilar-Benitez et al., Z.Phys. C40 (1988) 321.

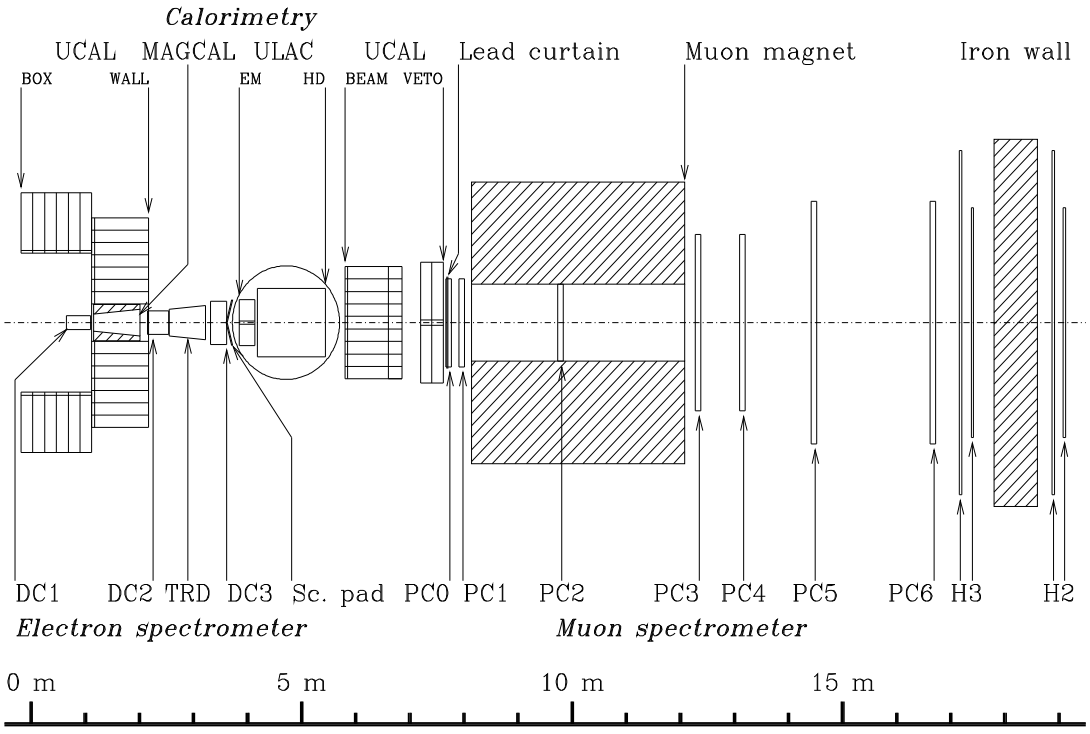

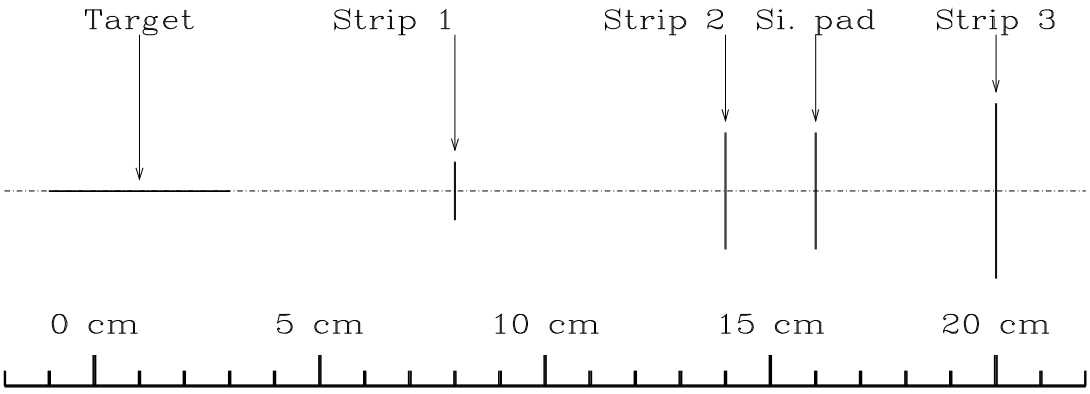

Figure 1: 1989 HELIOS apparatus

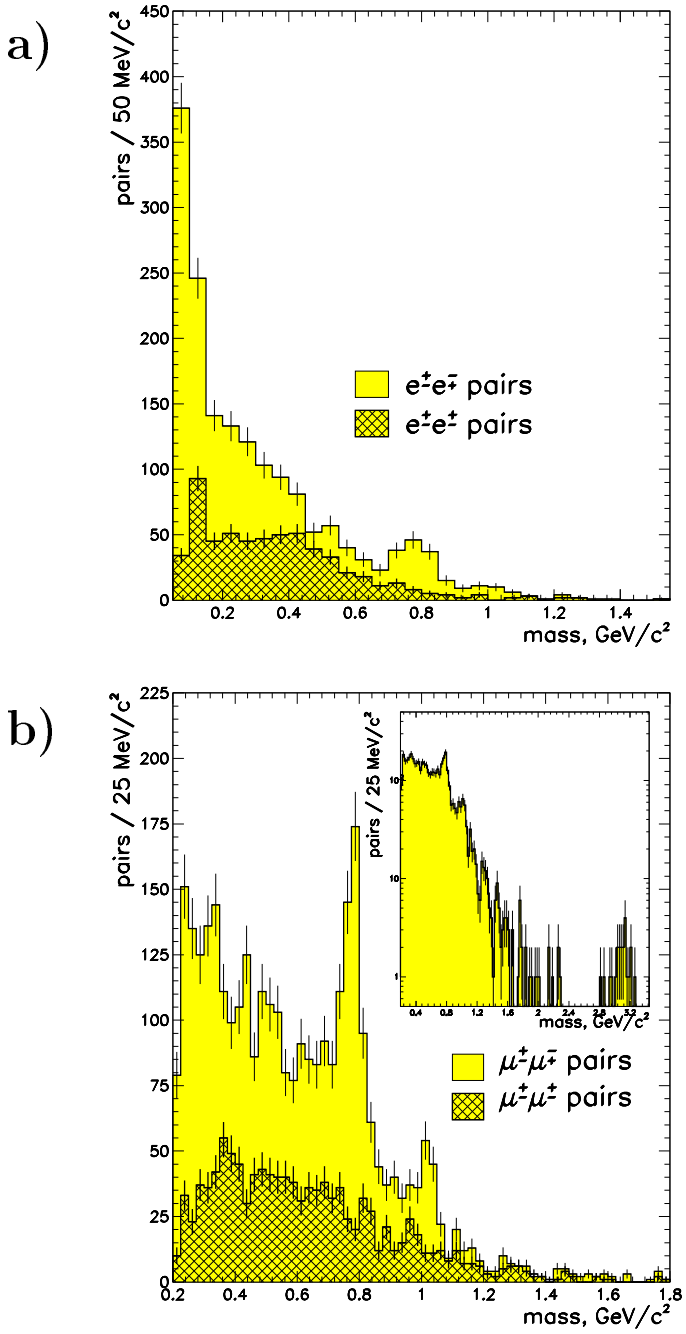

Figure 2: (a) Electron Pair Data Effective Mass Spectrum
(b) Muon Pair Data Effective Mass Spectrum. Inset figure shows all di-muon pairs.

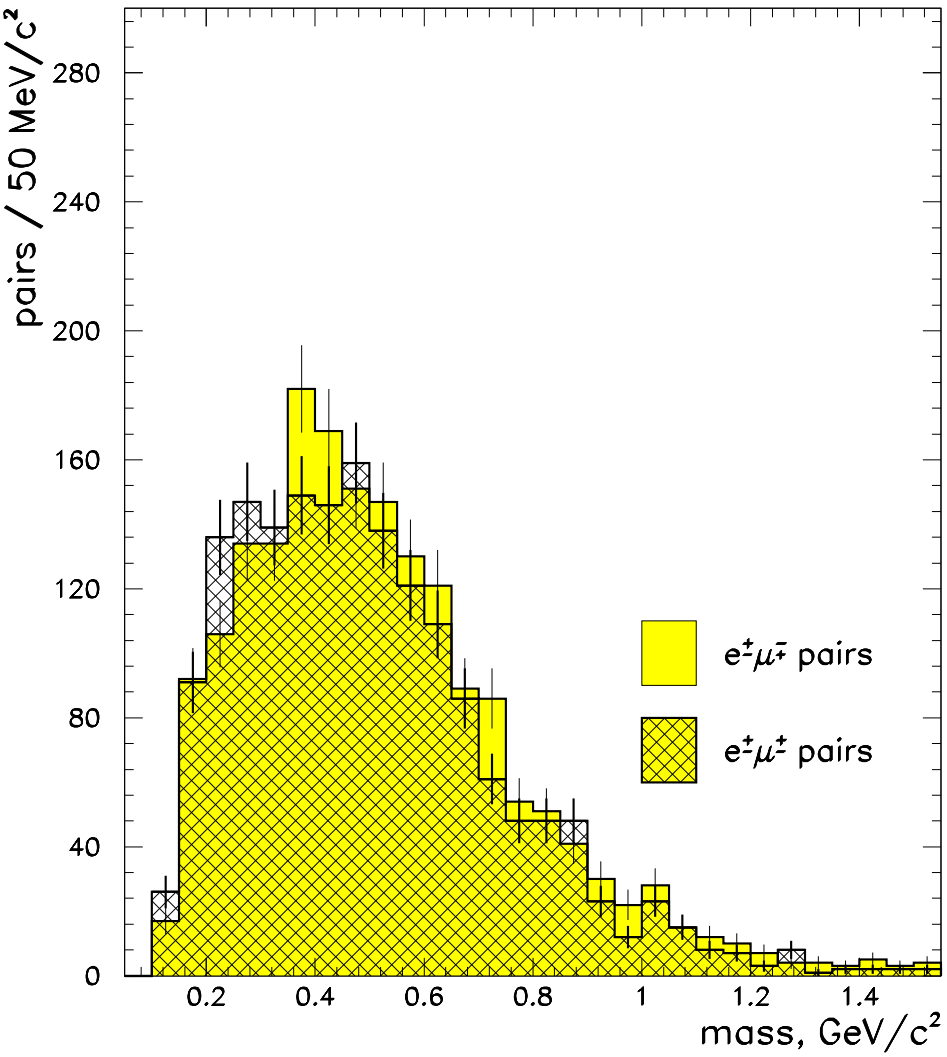

Figure 3: Electron-Muon Pair Data Effective Mass Spectrum

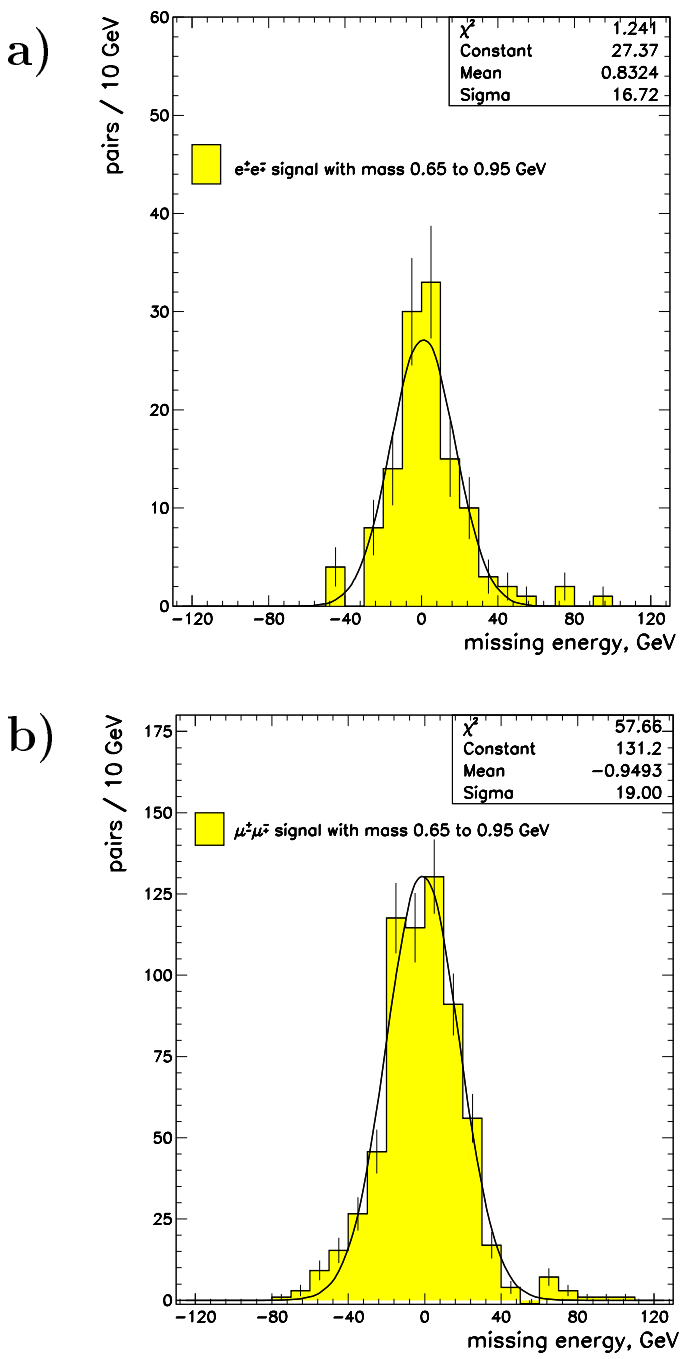

Figure 4: (a) Missing Energy Spectrum for ρ/ω Di-electrons
(b) Missing Energy Spectrum for ρ/ω Di-muons

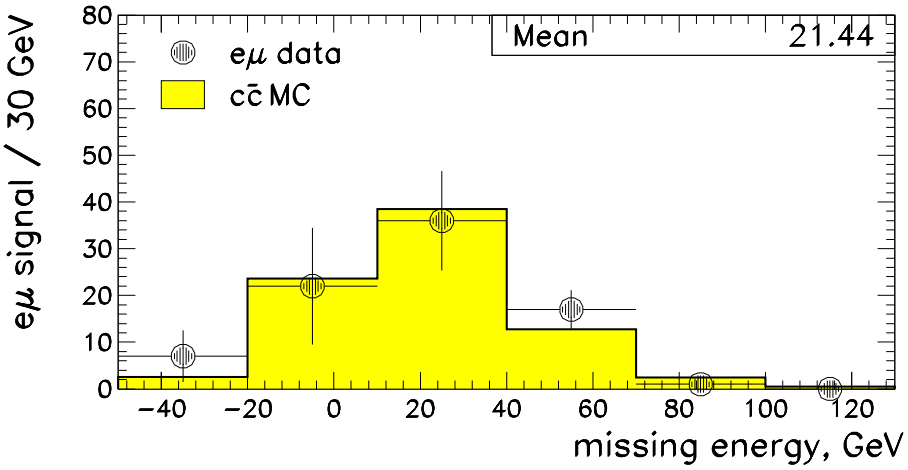

Figure 5: Missing Energy Spectrum for $e^{\pm}\mu^{\mp}$ Signal

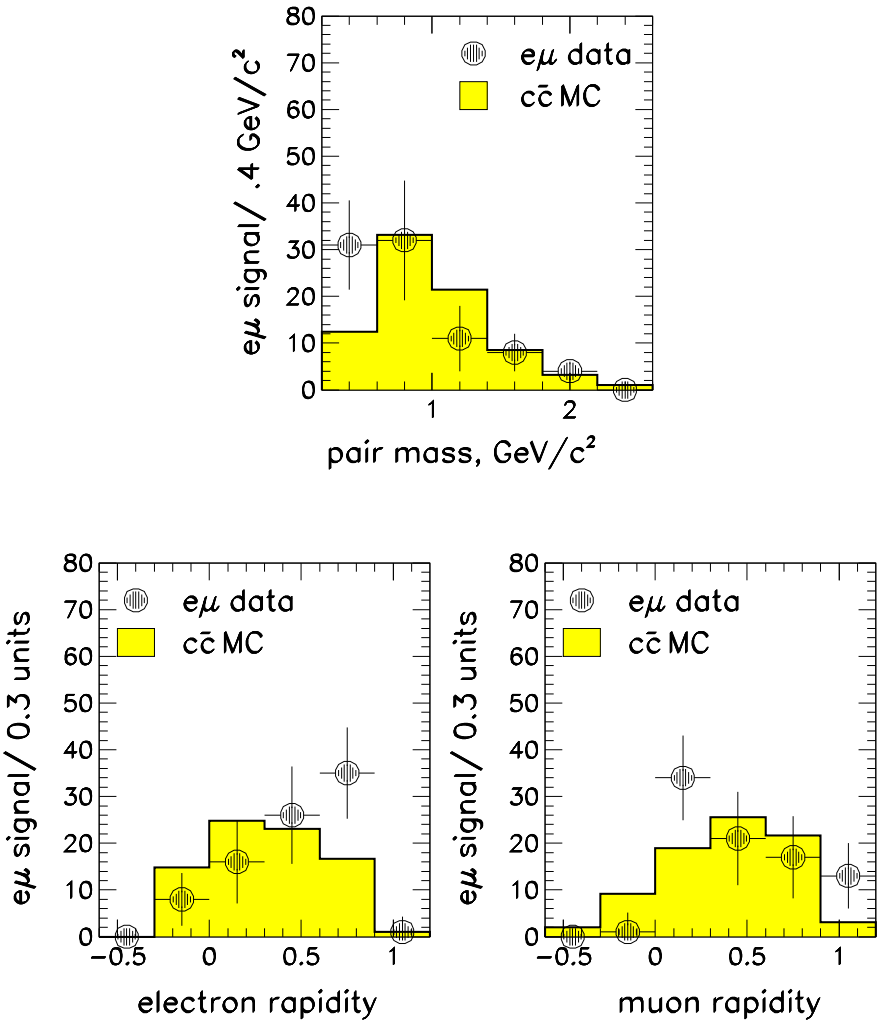

Figure 6: $e\mu$ Signal vs. $c\bar{c}$ Monte Carlo
Upper plot is pair effective mass. Lower left hand plot is electron rapidity , lower right hand plot is muon rapidity.

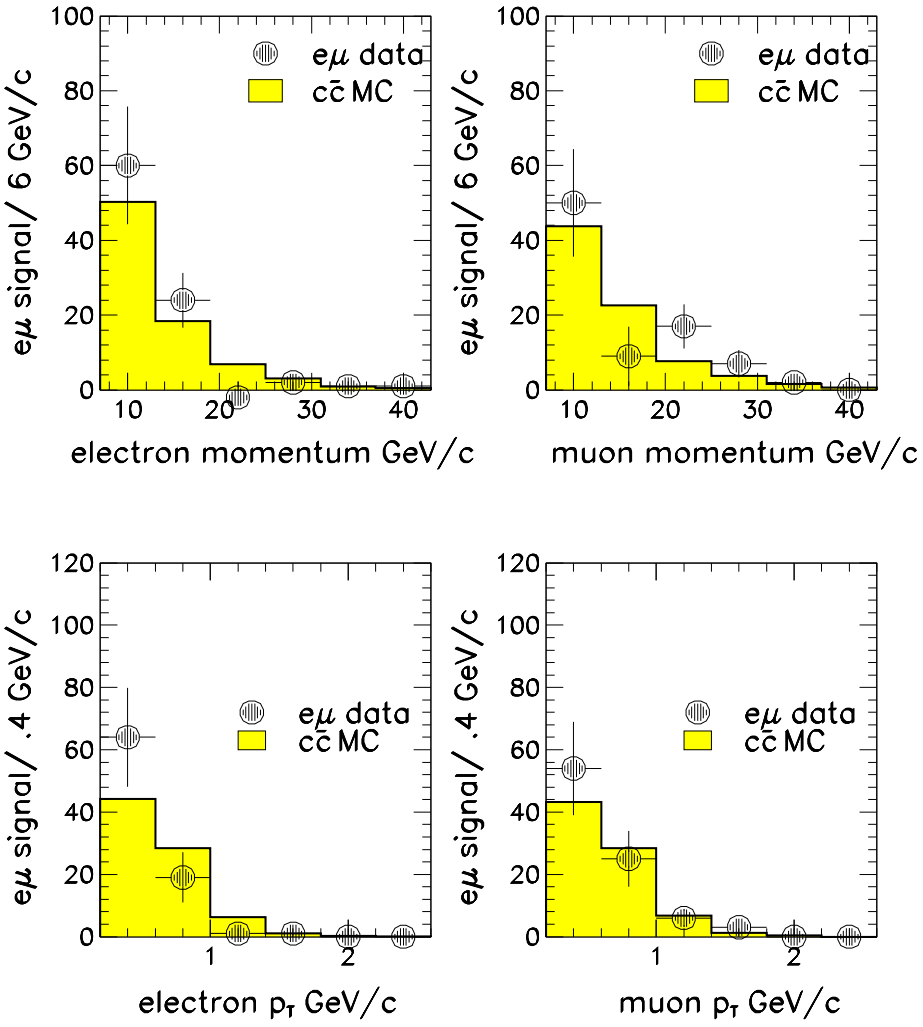

Figure 7: $e\mu$ Signal vs. $c\bar{c}$ Monte Carlo
Upper left hand plot is electron momentum, upper right hand plot is muon momentum. Lower left hand plot is electron transverse momentum, lower right hand plot is muon transverse momentum.